# IAC-02-A.6.09

# PRIMER VECTOR OPTIMIZATION: SURVEY OF THEORY, NEW ANALYSIS AND APPLICATIONS

**J.J. Guzmán, L.M. Mailhe, C. Schiff**
a.i. solutions, Inc.
Mission Design Division
Lanham, Maryland, USA

**S.P. Hughes, and D.C. Folta**
NASA Goddard Space Flight Center
Guidance, Navigation, and Control Center
Greenbelt, Maryland, USA

# 53rd International Astronautical Congress
# The World Space Congress - 2002
# 10-19 Oct 2002/Houston, Texas

# PRIMER VECTOR OPTIMIZATION: SURVEY OF THEORY, NEW ANALYSIS AND APPLICATIONS

J. J. Guzmán,[*] L.M. Mailhe,[†] C. Schiff[‡]
*a.i. solutions, Inc.*
*Lanham, MD 20706, USA*

S.P. Hughes[§] and D.C. Folta[¶]
*NASA Goddard Space Flight Center*
*Greenbelt, MD 20771, USA*

## Abstract

In this paper, a summary of primer vector theory is presented. The applicability of primer vector theory is examined in an effort to understand when and why the theory can fail. For example, since the Calculus of Variations is based on "small" variations, singularities in the linearized (variational) equations of motion along the arcs must be taken into account. These singularities are a recurring problem in analyses that employ "small" variations. Two examples, the initialization of an orbit and a line of apsides rotation, are presented. Recommendations, future work, and the possible addition of other optimization techniques are also discussed.

## Introduction

The work presented in this paper focuses on trajectory optimization using Lawden's primer vector theory.[1] Primer vector theory can be considered to be a byproduct of applying the Calculus of Variations (**COV**) to the problem of minimizing the fuel usage of impulsive trajectories. For an $n$-impulse trajectory, it involves the solution of $n-1$ two-point boundary value problems. The application of COV requires a path or initial guess to evaluate the variations. As a result, the analysis requires an a priori specification of the time of flight and/or an initial guess for the path. Therefore, this type of analysis is termed a *time-fixed problem*. However, variations in the endpoints might be allowed to explore neighboring solutions with different times of flight. In this paper, a general formulation of the primer vector is employed. Most importantly, the applicability of primer vector theory is examined in effort to understand when and why the theory can fail. Potential problems are discussed candidly to motivate further study and understanding. (Some examples are utilized to illustrate some of the issues.) Of course, one of the reasons for examining extreme cases is to develop software tools that can somehow "communicate" to the user potential problems. Understanding these problems, in turn, helps in developing robust tools that can be exploited for a variety of missions including single and multiple coordinated spacecraft. The addition of state dependent constraints is, however, not considered in this paper. Two examples, the initialization of an orbit and a line of apsides rotation, are presented. Recommendations, future work, and the possible addition of other optimization techniques are also discussed.

## Historical Background

The contributions in the area of trajectory optimization utilizing primer vector theory are numerous. The ones that were used for this investigation will be discussed here. Lawden applied COV techniques to the problem of optimizing rocket trajectories and coined the name "primer vector" for the adjoint vector variable associated with the velocity. Lawden recognized and exploited the significance of the primer vector and collected his work in a book.[1] (It should be remarked that other researchers also utilized COV for a variety of problems related to trajectory optimization.[2,3]) With primer vector theory, Lawden provided a set of necessary conditions for the fuel optimality of impulsive trajectories. In 1968, Lion and Handelsman extended the theory by developing methods to improve — in terms of fuel cost — non-optimal trajectories.[4] (In this context, non-optimal trajectories are those that do not meet the set of necessary conditions outlined by Lawden.) The methods developed by Lion and Handelsman

---

[*] Aerospace Engineer, guzman@ai-solutions.com
[†] Aerospace Engineer, mailhe@ai-solutions.com
[‡] Chief Scientist, schiff@ai-solutions.com
[§] Aerospace Engineer, shughes@pop500.gsfc.nasa.gov
[¶] Senior Aerospace Engineer, dfolta@pop500.gsfc.nasa.gov

included adding an impulse and coasting along the initial and final orbits. Perhaps more importantly, their work extended the theory to "find" the optimal number of impulses. Utilizing Lawden's work and with the concepts from Lion and Handelsman, Jezewski and Rozendaal developed an efficient algorithm for calculating $n$-impulse trajectories.[5] The paper by Jezewski and Rozendaal also contains a clever combination with a direct method (Fletcher-Powell modified descent) to achieve optimality in the primer vector sense. Furthermore, Jezewski and Faust also considered adding constraints.[6] Jezewski collected his work in a NASA technical report.[7] The extensive work by Prussing[8-14] has provided much needed insight into the orbit to orbit and/or rendezvous transfer problem. Then, the work by Hiday and Howell has elegantly extended the theory (the previous references are in the two-body problem, **2BP**) to transfers between libration point orbits in the elliptic restricted three-body problem (**ER3BP**).[15,16] In this investigation, interest is in understanding, applying, and extending primer vector theory to create robust software tools that can be used for the new set of upcoming challenging missions. These missions might include regimes such as Earth orbiting platforms (including orbits that might have high eccentricity), Moon orbiters, libration point orbiters and other deep space probes. Clearly, understanding how and when the theory can be applied is critical.

## Primer Vector Theory

In this section, a general formulation of primer vector theory — based on a general force model that might be expressed in a rotating frame[15] — is employed to review the theory.

### Equations of Motion

Consider a general case where the spacecraft nonlinear equations of motion are given by,

$$\ddot{\bar{r}} = \bar{g}(t, \bar{r}, \dot{\bar{r}}) + \Gamma \hat{u}_T, \qquad (1)$$

where $\Gamma$ and $\hat{u}_T$ are the thrust acceleration magnitude and unit direction respectively. The function $g$ is referred to as the *coastal acceleration*. Letting $T$ equal the thrust force and $m$ the spacecraft mass, $\Gamma = T/m$. Furthermore, letting $\bar{v} = \dot{\bar{r}}$, Equation (1) in state space form is given by,

$$\left\{ \begin{array}{c} \dot{\bar{r}} \\ \dot{\bar{v}} \end{array} \right\} = \left\{ \begin{array}{c} \bar{v} \\ \bar{g}(t, \bar{r}, \bar{v}) + \Gamma \hat{u}_T \end{array} \right\}. \qquad (2)$$

These are the nonlinear, first order differential equations.

*Linearization*

For coast arcs, i.e., null thrust arcs (**NT arcs**), Equation (2) can be linearized about some reference path as follows,

$$\left\{ \begin{array}{c} \delta\dot{\bar{r}} \\ \delta\dot{\bar{v}} \end{array} \right\} = A(t)|_{\text{ref}} \left\{ \begin{array}{c} \delta\bar{r} \\ \delta\bar{v} \end{array} \right\}, \qquad (3)$$

where $A$ is the Jacobian matrix,

$$A(t) = \left[ \begin{array}{cc} 0 & I \\ G_r & G_v \end{array} \right], \qquad (4)$$

and, where $G_r = \frac{\partial \bar{g}}{\partial \bar{r}}$ and $G_v = \frac{\partial \bar{g}}{\partial \bar{v}}$. The linear system in Equation (3) has the following solution,

$$\left\{ \begin{array}{c} \delta\bar{r} \\ \delta\bar{v} \end{array} \right\} = \Phi(t, t_o) \left\{ \begin{array}{c} \delta\bar{r}_o \\ \delta\bar{v}_o \end{array} \right\}, \qquad (5)$$

where $\Phi(t, t_o)$ is the state transition matrix (**STM**) from $t_o$ to $t$ *along the reference path*,

$$\Phi = \left[ \begin{array}{cc} \Phi_{rr}(t, t_o) & \Phi_{rv}(t, t_o) \\ \Phi_{vr}(t, t_o) & \Phi_{vv}(t, t_o) \end{array} \right]. \qquad (6)$$

Depending on the regime, analytical (or approximate) STMs might be available. Nevertheless, for generality, the STM should be numerically integrated. This presents no significant computational speed problem in today's computers.

### Rocket Engine Definition

The solution of the rocket equation[17] in field-free space yields the following equation for the change in velocity, or $\Delta v$

$$\Delta v = c_{\text{ev}} \ln \left( \frac{m_o}{m_f} \right), \qquad (7)$$

where $c_{\text{ev}}$ is the rocket's effective exhaust velocity and $m_o$ and $m_f$ are the initial and final masses respectively. From conservation of mass, the mass flow rate is given by

$$\dot{m} = -T/c_{\text{ev}}, \qquad (8)$$

where $T$ is the thrust magnitude. For a realistic rocket engine, the mass flow rate is limited. As a result, there is a maximum attainable thrust, $\tilde{T}$, that can be achieved. This maximum thrust is given by

$$\tilde{T} = -c_{\text{ev}} \dot{m}_{\text{max}} \qquad (9)$$

Thus, $0 \leq T \leq \tilde{T}$. This can be transformed into an equality constraint,[15]

$$T(\tilde{T} - T) - q^2 = 0, \qquad (10)$$

where $q \geq 0$.

2

## Optimal Control Problem Formulation

As an optimal control problem, and to minimize the total fuel usage, the problem can be stated as, minimize

$$J = c_{ev} \ln\left(\frac{m_o}{m_f}\right), \qquad (11)$$

subject to the differential constraints (state equations),

$$\dot{\bar{r}} = \bar{v}, \qquad (12a)$$

$$\dot{\bar{v}} = \bar{g}(t, \bar{r}, \bar{v}) + \Gamma \hat{u}_T, \qquad (12b)$$

$$\dot{m} = -\frac{T}{c_{ev}}, \qquad (12c)$$

and to the control constraints,

$$\|\hat{u}\| = 1, \qquad (13a)$$

$$T(\tilde{T} - T) - q^2 = 0. \qquad (13b)$$

The above cost function and constraints formulation is sometimes referred to as the *problem of Mayer*. (In this case, control equality constraints have been added.) The interested reader will find an excellent COV reference in the book by Citron.[18] It should be remarked that the addition of path constraints augments the cost function. As a result, *the addition of constraints requires modifications in primer vector theory.*[12]

### *Hamiltonian*

If the maximum principle* is utilized, the Hamiltonian function is defined as,

$$H = \bar{\lambda}^T \bar{f} - L, \qquad (14)$$

where $\bar{\lambda}$ is an unknown vector of Lagrange multipliers (co-state variables), $\bar{f}$ is a vector containing the system equations, and $L$ is the integrand in the cost function or index of performance. For the current problem formulation, $\bar{f} = \{\dot{\bar{r}}, \dot{\bar{v}}, \dot{m}\}^T$ and $L = 0$. Therefore, the Hamiltonian is given by

$$H = \bar{\lambda}_r^T \bar{v} + \bar{\lambda}_v^T \left(\bar{g} + \frac{T}{m}\hat{u}_T\right) - \lambda_m \frac{T}{c_{ev}}. \qquad (15)$$

For NT arcs, $T = 0$ and $H$ is given by,

$$H_{NT} = \bar{\lambda}_r^T \bar{v} + \bar{\lambda}_v^T \bar{g}. \qquad (16)$$

It can also be shown that the time derivative of Equation (16) is given by,[15]

$$\dot{H}_{NT} = \bar{\lambda}_v^T \frac{\partial \bar{g}}{\partial t}. \qquad (17)$$

---

*Pontryagin's maximum (or minimum) principle can be derived by utilizing COV in a problem formulation that includes control variables. It can be shown that the maximum principle is equivalent to the Weierstrass condition.[18]

Therefore, *if g is not an explicit function of time*, $\frac{\partial \bar{g}}{\partial t} = 0$ *and a first integral exists*. That is, $H_{NT} =$ constant. In rotating frames, under an inverse-square gravitational field, a first integral exists if the frame is rotating at a constant rate in the inertial frame.

### Primer Necessary Conditions

Considering the optimal control problem formulation and applying COV (or the maximum principle†) and letting the co-state vector associated with the velocity, $\bar{\lambda}_v$ be equal to $\bar{p}$, yields the following necessary conditions:

1. The primer evolution is governed by

$$\ddot{\bar{p}} = (G_r - \dot{G}_v)^T \bar{p} - G_v^T \dot{\bar{p}}. \qquad (18)$$

2. During transfers $\|\bar{p}\| = p <= 1$, with impulses at instants for which $p = 1$.

3. At an impulse time $\bar{p} = \hat{p} = \hat{u}_T^*$, where $\hat{u}_T^*$ is the optimal thrust direction.

4. At all interior impulses (not at the initial or final times) $\bar{p} \cdot \dot{\bar{p}} = 0$. This condition has implications on the slope of the primer vector magnitude since

$$\frac{d\|\bar{p}\|}{dt} = \frac{d}{dt}(\bar{p} \cdot \bar{p})^{1/2} = \frac{\dot{\bar{p}} \cdot \bar{p}}{\|\bar{p}\|}.$$

Therefore, $\frac{d\|\bar{p}\|}{dt} = 0$ at the intermediate impulses. Also, for convenience, let $\dot{p} = \frac{d\|\bar{p}\|}{dt}$.

These conditions are necessary (but not sufficient) for an optimal trajectory (time-fixed problem). In this paper, a trajectory that meets the above conditions will be called an optimal trajectory.

### Primer Vector Evolution

Consider the first primer condition as expressed in Equation (18). If the following two conditions‡ are met,

$$(G_r - \dot{G}_v)^T = G_r \text{ and} \qquad (19a)$$

$$G_v^T = -G_v, \qquad (19b)$$

then the primer equations are given by,

$$\left\{\begin{array}{c} \dot{\bar{p}} \\ \ddot{\bar{p}} \end{array}\right\} = \left[\begin{array}{cc} 0 & I \\ G_r & G_v \end{array}\right] \left\{\begin{array}{c} \bar{p} \\ \dot{\bar{p}} \end{array}\right\}. \qquad (20)$$

---

†Lawden applied the calculus of variations. Alternatively, these conditions can be derived utilizing the maximum principle.

‡These conditions are a result of the kinematics of the problem.

In this case the spacecraft linearized equations of motion have the same form as the primer differential equations. In fact, the time histories of $G_r(t)$ and $G_v(t)$ do not depend on the primer vector. As a result, the primer vector solution is,

$$\left\{ \begin{array}{c} \bar{p} \\ \dot{\bar{p}} \end{array} \right\} = \left[ \begin{array}{cc} \Phi_{rr}(t,t_o) & \Phi_{rv}(t,t_o) \\ \Phi_{vr}(t,t_o) & \Phi_{vv}(t,t_o) \end{array} \right] \bigg|_{ref} \left\{ \begin{array}{c} \bar{p}_o \\ \dot{\bar{p}}_o \end{array} \right\}, \quad (21)$$

where the STM blocks are evaluated along the reference path and the initial conditions, $(\bar{p}_o, \dot{\bar{p}}_o)$, are still required. These will be obtained by considering the arc boundaries. Before that, the theory of adjoint systems is briefly examined.

*Adjoint System*

There is a complete theory of adjoint systems that utilizes the concept of adjoint differential forms.[18] Suppose that a linear system is given by,

$$\dot{\bar{Z}} = A(t)\bar{Z}, \quad (22)$$

then, an adjoint system to the above one is given by

$$\dot{\bar{\phi}} = -A^T(t)\bar{\phi}, \quad (23)$$

where $T$ is the transpose. Let $A(t)$ be the Jacobian matrix, Equation (4), and let

$$\bar{Z} = \left\{ \begin{array}{cc} \delta\bar{r} & , & \delta\bar{v} \end{array} \right\}^T, \quad (24)$$

$$\bar{\phi} = \left\{ \begin{array}{cc} \bar{\phi}_r & , & \bar{\phi}_v \end{array} \right\}^T. \quad (25)$$

Then,

$$\left\{ \begin{array}{c} \dot{\bar{\phi}}_r \\ \dot{\bar{\phi}}_v \end{array} \right\} = \left[ \begin{array}{cc} 0 & -G_r^T \\ -I & -G_v^T \end{array} \right] \left\{ \begin{array}{c} \bar{\phi}_r \\ \bar{\phi}_v \end{array} \right\}, \quad (26)$$

is the adjoint system to the linearized system in Equation (3). Then, taking the derivative of the equation for $\dot{\bar{\phi}}_v$ and using the equation for $\dot{\bar{\phi}}_r$,

$$\ddot{\bar{\phi}}_v = (G_r - \dot{G}_v)^T \bar{\phi}_v - G_v^T \dot{\bar{\phi}}_v. \quad (27)$$

Thus, the adjoint differential equations and the primer vector differential equations (18) are the same for an NT arc. *This fact has implications in the behavior and applicability of primer vector theory.*

Another interesting fact is that, from the definition of an adjoint system, it can be shown that,

$$\bar{\phi}^T \bar{L}(\bar{Z}) - \bar{Z}^T \bar{M}(\bar{\phi}) = \frac{d}{dt} \left( \bar{\phi}^T \bar{Z} \right), \quad (28)$$

where $\bar{L}(\bar{Z})$ and $\bar{M}(\bar{\phi})$ are vectors of linear differential forms given by

$$\bar{L}(\bar{Z}) = \dot{\bar{Z}} - A(t)\bar{Z}, \quad (29)$$

$$\bar{M}(\bar{\phi}) = -\dot{\bar{\phi}} - A^T(t)\bar{\phi}, \quad (30)$$

in this case, $\bar{L}(\bar{Z}) = \bar{M}(\bar{\phi}) = 0$, therefore,

$$\bar{\phi}^T \bar{Z} = \text{constant.} \quad (31)$$

So,

$$\bar{\phi}_r^T \delta\bar{r} + \bar{\phi}_v^T \delta\bar{v} = \text{constant.}$$

Letting $\bar{\phi}_v = \bar{p}$ and utilizing the second equation in (26),

$$\bar{\phi}_r = -(\dot{\bar{p}}^T + G_v^T \bar{p}).$$

Thus,

$$-(\dot{\bar{p}}^T + \bar{p}^T G_v)\delta\bar{r} + \bar{p}^T \delta\bar{v} = \text{constant.} \quad (32)$$

This equation was employed by Lion and Handelsman when considering contemporaneous variations of the cost function.[4] It has been derived in an inertial frame in the 2BP by Jezewski[7] and in rotating frame in the ER3BP by Hiday.[15] To distinguish this equation from the adjoint or co-state equations, call it the *variational adjoint equation*[§]. It is very useful when considering different variations of the cost function to improve the trajectory.

**Impulsive Maneuvers**

At the impulses the primer vector is given by

$$\bar{p} = \frac{\Delta\bar{v}}{||\Delta\bar{v}||} = \Delta\hat{v}. \quad (33)$$

Now, suppose there is an arc from $t_o$ to $t_f$ with an impulse at $t_o$ and an impulse at $t_f$ and no thrust in between. Then,

$$\bar{p}_o = \Delta\hat{v}_o, \quad (34\text{a})$$

$$\bar{p}_f = \Delta\hat{v}_f. \quad (34\text{b})$$

To obtain the primer vector time history in between the impulses, Equation (21) is used. Nevertheless, the primer vector slope $\dot{\bar{p}}_o$ at $t_o$ is needed. Utilizing the first equation in Equation (21) and evaluating at $t = t_f$,

$$\dot{\bar{p}}_o = \Phi_{rv}^{-1}(t_f, t_o)[\bar{p}_f - \Phi_{rr}(t_f, t_o)\bar{p}_o], \quad (35)$$

provided $\Phi_{rv}^{-1}(t, t_o)$ is defined (i.e., $\Phi_{rv}$ is nonsingular). If the nominal path and the initial and final times are known, the STM is readily available. As a result, no iteration is needed. Alternatively, a shooting method can be applied to the two point boundary value problem given by initially guessing $\dot{\bar{p}}_o$ and using Equations (20) and (34).

---

[§]Jezewski and Hiday call this equation the *adjoint equation.*

4

## Improving Non-Optimal Trajectories

Improving non-optimal trajectories using primer vector theory is the main contribution of Lion and Handelsman.[4] Essentially, first order variations of the cost function (i.e., $\Delta v_{\text{total}}$ in the impulsive approximation) are considered for different perturbed trajectories.[4,5,15]

### Impulses and Continuous Quantities

For the cost function variations, it is of interest to understand what quantities are continuous across an impulse. The time and the position vector are, of course, continuous but not the velocity. The velocity discontinuity is due to the application of the impulsive maneuver. Thus, for a mid-impulse, $\Delta \bar{v}_m = \bar{v}_m^+ - \bar{v}_m^-$. Therefore, the coastal acceleration (i.e., $\bar{g} = \bar{g}(t, \bar{r}, \bar{v})$) is not continuous across an impulse. Nevertheless, suppose that

$$\bar{g}(t, \bar{r}, \bar{v}) = \bar{g}_1(t, \bar{r}) + \bar{g}_2(t, \bar{v}), \qquad (36)$$

where the $\bar{g}_1$ and $\bar{g}_2$ vector functions are force model dependent. If $\bar{g}_2$ can be expressed as

$$\bar{g}_2(t, \bar{v}) = G_v \bar{v}, \qquad (37)$$

where $G_v = \frac{\partial \bar{g}}{\partial \bar{v}} = \frac{\partial \bar{g}_2}{\partial \bar{v}}$, then, Equation (36) can be written as,

$$\bar{g}(t, \bar{r}, \bar{v}) - G_v \bar{v} = \bar{g}_1(t, \bar{r}). \qquad (38)$$

Since $\bar{g}_1$ is a function of time and position only, across an impulse,

$$(\bar{g} - G_v \bar{v})|_+ = (\bar{g} - G_v \bar{v})|_- . \qquad (39)$$

*If Equation (39) and the variational adjoint Equation (32) are satisfied, then the cost function variations presented next can be utilized.*

### Criteria for Three Impulses

Perturb a two-impulse arc with the addition of a mid-impulse at some time, $t_m$, and position $\bar{r}_m + \delta \bar{r}_m$. (The position $\bar{r}_m$ is the position along the unperturbed path at $t_m$.) The initial and the final times and positions, $(t_o, \bar{r}_o)$ and $(t_f, \bar{r}_f)$, are fixed. Define the cost function variation as $\delta J = J' - J$, where $J'$ is the fuel cost on the perturbed trajectory. Then, considering first order terms only, it can be shown that

$$\delta J = c(1 - \bar{p}_m^T \hat{\eta}), \qquad (40)$$

where the following are mid-impulse parameters: $c$ is the magnitude of the impulse, $\bar{p}_m$ is the primer vector at $t_m$ and $\hat{\eta}$ is an unit vector in the direction of the impulse. Then, for an improvement in

cost, $\delta J < 0$. Thus, using the definition of a dot product, if $\|\bar{p}_m\| > 1$ at any time, a third impulse is beneficial. Furthermore, the greatest decrease in the cost function will be achieved if the impulse is applied at the maximum of $\|\bar{p}_m\|$ at time $t_m$ and in the direction of $\hat{\eta}$. The position along the perturbed path and the magnitude of the impulse are yet to be determined.

### Calculation of the Interior Impulse

Consider finding the position of the impulse. Utilizing the fact that the position across an impulse is continuous, using the STM before and after the impulse, and utilizing the information obtained from Equation (40), gives the following variational equation,

$$\delta \bar{r}_m = c \tilde{A}^{-1} \frac{\bar{p}_m}{\|\bar{p}_m\|}, \qquad (41)$$

where

$$\tilde{A} = \Phi_{vv}(t_m, t_f) \Phi_{rv}(t_m, t_f)^{-1} \\ - \Phi_{vv}(t_m, t_o) \Phi_{rv}(t_m, t_o)^{-1}.$$

This equation, of course, is valid only for non-singular $\tilde{A}$ and determines the position of the mid-impulse[¶]. Now, to estimate the magnitude, $c$, of the impulse, the expression for the cost on the perturbed path, $J'$, can be expressed as a function of $c$ and minimized. Two estimates are presented in the literature in terms of the order of the cost variational that is minimized. Specifically, Jezewski and Rozendaal[5] retain up to second order terms and obtain an analytical approximation, while Hiday uses the exact expression and solves for the minimum iteratively. The first estimate is appropriate for most applications in the two-body problem while the second is more general and perhaps better for a robust tool. In any case, the mid-impulse should decrease the cost but might not produce an optimal trajectory in the sense of Lawden. The subsequent optimization of the three-impulse trajectory is presented next.

### Convergence to the Optimal Trajectory

For a three-impulse arc, if the *time and position* of the mid-impulse are allowed to vary, it can be shown that,

$$\delta J = (\Delta \dot{\bar{p}}_m)^T d\bar{r}_m + (\Delta H_m) dt_m \qquad (42)$$

where $\Delta \dot{\bar{p}}_m$ and $\Delta H_m$ are, respectively, the primer vector and the Hamiltonian differences at the impulse. If the trajectory is indeed optimal, the first

----

[¶]Not surprisingly, Equation (41) appears in differential correction schemes for position continuity. Compare, for instance, the $M_p$ matrix in equation 15 of Pernicka and Howell[19] with $\tilde{A}$ above.

cost variation must vanish. Thus, it is required that, $\Delta \dot{\bar{p}}_m = \bar{0}$ and, $\Delta H_m = 0$. It can be shown that $\Delta H_m = \dot{\bar{p}}_m^{-T} \bar{v}_m^- - \dot{\bar{p}}_m^{+T} \bar{v}_m^+$. (In this paper, for the primer vector data figures, let the scalar $\tilde{H}$ be given by $\dot{\bar{p}}^T \bar{v}$.) In an interesting "mix", a direct optimization method can be applied to vary the mid-impulse time and position to meet the above conditions. In this investigation, following Hiday,[15] the Broyden-Fletcher-Goldfarb-Shanno, **BFGS**, algorithm is utilized.

An additional complication might appear if after solving for the time and position of the mid-impulse, the primer vector history exceeds unity at some point. In that case, an additional impulse must be implemented. Hiday remarks that in the ER3BP, each additional impulse is solved for one at a time to avoid "destroying the integrity of the numerical solutions" for the initial and final orbits. Thus, if $K$ additional impulses are needed, $K$ BFGS minimizations of Equation (42) are performed. In the 2BP, however, it is possible to compute the times and positions of all the additional impulses simultaneously. Thus, a single function of $4K$ variables is minimized.[5]

*Varying the Endpoints*

So far the trajectory has been optimized by adding additional impulses while keeping the endpoints' times (and thus, the positions) fixed. Not surprisingly, additional improvement is possible by varying these times. The general expression for time variations at both endpoints is given by,[15]

$$\delta J = -\dot{p}_o \|\Delta \bar{v}_o\| dt_o - \dot{p}_f \|\Delta \bar{v}_f\| dt_f, \qquad (43)$$

where the initial and final time variations be given by $dt_o$ and $dt_f$, respectively. Furthermore, the initial and final primer magnitude slopes are given by $\dot{p}_o$ and $\dot{p}_f$, respectively. Now, to have a lower cost, $\delta J$ in Equation (43) must be less than zero. If the following terminology is defined, 1) initial coast ($dt_o > 0$), 2) early departure ($dt_o < 0$), 3) final coast ($dt_f < 0$), and, 4) late arrival ($dt_f > 0$); then, the following four cases cover all the non-zero primer slope combinations,

- If $\dot{p}_o > 0$ and $\dot{p}_f < 0 \Rightarrow$ Apply Initial Coast and Final Coast.

- If $\dot{p}_o > 0$ and $\dot{p}_f > 0 \Rightarrow$ Apply Initial Coast and Late Arrival.

- If $\dot{p}_o < 0$ and $\dot{p}_f < 0 \Rightarrow$ Apply Early Departure and Final Coast.

- If $\dot{p}_o < 0$ and $\dot{p}_f > 0 \Rightarrow$ Apply Early Departure and Late Arrival.

Again, see Hiday for details.[15] Of course, if the slopes are zero, no further improvement is achieved by varying the endpoints' times.

## Applicability of Primer Vector Theory

Two issues that cause problems in the application of primer vector theory have been observed in this investigation. *First*, recall that the primer vector system in Equation (18) is adjoint to the linear system in Equation (3). Moreover, the primer vector differential equations and the (linear) variational equations of motion have the same form. As a result, the primer vector and its derivative follow Equation (21). Unfortunately, depending on the force model, on the flight regime (e.g. circular or eccentric orbit), and on the length of the propagation, the linearized dynamics might not be adequate to represent the natural dynamics of the system. That is, "small" variations might not remain "small" and solving for the primer vector history becomes numerically intractable. *Second*, there might be isolated points along the nominal path or orbit where the upper right hand block of the STM, $\Phi_{rv}$, is singular. This singularity prevents the computation of the initial primer derivative via Equation (35) (the initial vector derivative is needed to use Equation (21) for the primer vector history). Next, these two issues are examined more carefully.

### Linear Theory Range

The first issue deals with the sensitivity of the linearized system in Equation (3). Specifically, interest is in understanding how "close" the solution of this system, i.e., Equation (5), is to the nonlinear system solution (numerically propagated). Recall, that the primer vector magnitude is equal to 1 at the places where impulses are applied. Then, it turns out that an *ad-hoc* test could be done in the following way:

1. Perturb the initial state as follows,

$$\left\{ \begin{array}{c} \delta \bar{r}_o \\ \delta \bar{v}_o \end{array} \right\} = d \left\{ \begin{array}{c} \bar{r}_o \\ \bar{v}_o \end{array} \right\}, \qquad (44)$$

where $d$ is a positive scalar such that $0 < d << 1$.

2. The magnitude of $\delta \bar{r}_o$ is required to be a "small" number, say 1 unit of length (for the cases that will be considered). That is, if $\|\delta \bar{r}_o\| = d \|\bar{r}_o\| = 1$, then $d = 1/\|\bar{r}_o\|$.

3. Propagate the path of interest using two methods: i) with the STM (integrated along the nominal orbit) and ii) numerically integrating the nonlinear system.
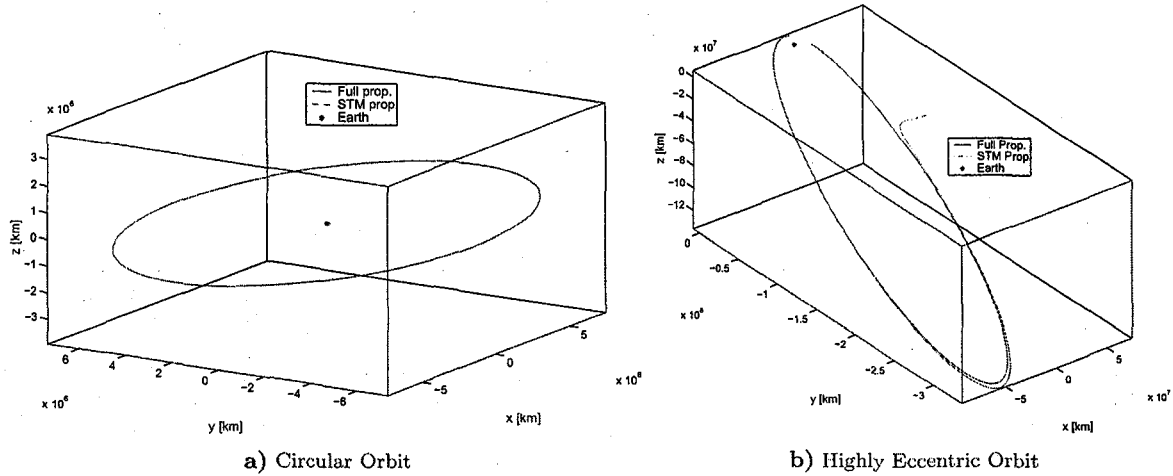
a) Circular Orbit　　　　　　　　b) Highly Eccentric Orbit

**Fig. 1　Linear and NonLinear Propagation**

Comparing how "close" the final states are in the integrations (last step) gives a rough estimate of the numerical sensitivity of the problem. For example, consider the following two cases in the two-body problem: 1) a circular orbit at a 1,500 km altitude (low Earth orbit) propagated for .5 days (about 5 revolutions), and 2) a highly eccentric orbit, e = 0.95, with a perigee altitude of 2,703 km propagated for 9.2 days[‖]. For both cases, the magnitude of the perturbed position vector is $\|\delta \bar{r}_o\| = 1$ km. The magnitude of the perturbed velocity vectors, $\|\delta \bar{v}_o\|$, are 0.000903 and 0.001019 km/sec, respectively. See Figure 1 for qualitative results. The results illustrate how for the highly eccentric orbit the STM propagation breaks down before one complete revolution. The onset of the "breakdown" takes place as the spacecraft approaches perigee and the cartesian STM changes very quickly. This type of behavior creates serious numerical problems in trying to obtain the primer vector history between periapsis points. Switching to a different formulation, e.g. orbital elements, might alleviate this problem. Schemes that utilize linear propagation for targeting and/or Monte Carlo analyses should investigate the linear theory range for all initial conditions.[21]

## Isolated Singularities

Moreover, there might be singularities (in the upper right hand block of the STM, $\Phi_{rv}$) at some specific points along the orbit. Singularities in the 2BP elliptic arcs occur when:

1. The difference between the initial and final

-----------------

[‖]This case was obtained from the Microwave Anisotropy (MAP) mission nominal orbit after it first perigee maneuver.[20]

times is a multiple of the reference orbit period.

2. The difference between the initial and final true anomalies are given by $k\pi$, for $k = 0, 1, 2, 3, \ldots$ — note that this covers the first case, thus, the additional singularities occur when the difference between the initial and final true anomalies given by $(2k+1)\pi$, for $k = 0, 1, 2, 3, \ldots$, and

3. The time of flight is a minimum for the given difference in true anomaly.

The above conditions are detailed in the 1964 report by Stern.[22] According to Stern, the first two are readily explained on physical grounds while the third is a consequence of the initial assumption of a linearized model. In the first case, the initial and final position perturbations are not independent. In the second case, the out-of-plane components are not independent. (Thus, specifying the transfer plane and considering only planar variations can remedy this situation.) The third case is more complex and depends on the eccentricity of the reference orbit as well as on the initial and final eccentric anomalies ($E_o$ and $E_f$). Stern shows that for this third case the following expression vanishes at the singularity points,

$$X = (3E_M - e\sin E_M \cos E_P)(\cos E_M + e\cos E_P)$$
$$-4\sin E_M, \tag{45}$$

where $E_M = \frac{1}{2}(E_f - E_o)$, and $E_P = \frac{1}{2}(E_f + E_o)$. Figure 2(a) displays a plot of $X$ versus number of revolutions for various eccentricities (0, 0.25, 0.5, 0.75). For the cases shown, the first crossing occurs after 1 revolution. See Figure 2(b) for a closer view at the crossing points. Therefore, as Stern remarks,
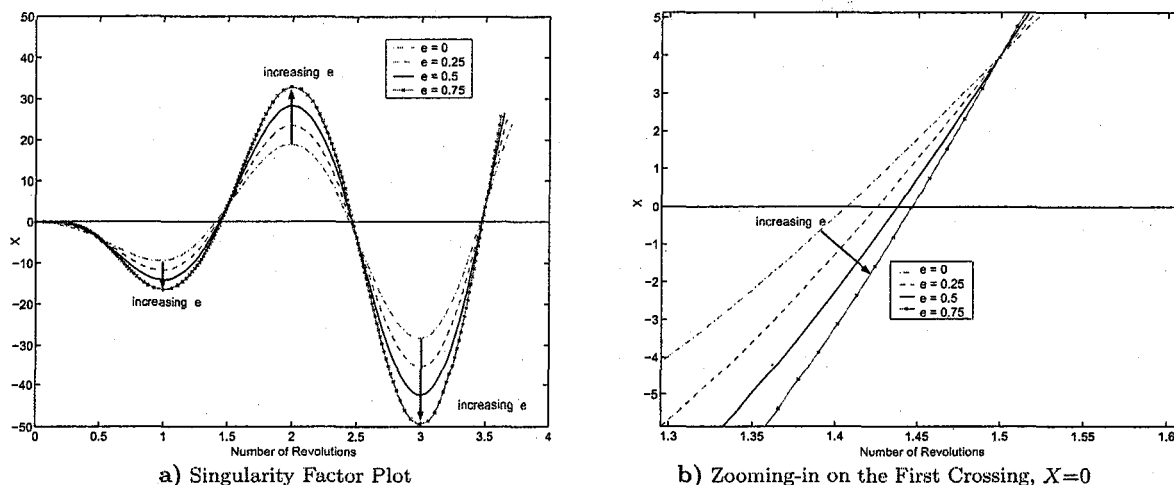
7

a) Singularity Factor Plot        b) Zooming-in on the First Crossing, $X=0$

**Fig. 2  Singularity Factor vs Number of Revolutions**

there are no singularities (of any type) for true anomaly differences greater than 0 degrees and less than 180 degrees. Nevertheless, general tools should be able to handle other cases that might include multiple revolutions. In fact, these multiple revolution cases allow the designers to use the concept of "phasing" orbits when implementing orbit transfers and/or rendezvous.[23] For a mission designer, these phasing orbits provide more opportunities to plan and execute maneuvers to correct errors (such as launch vehicle injection errors, implementation errors, thruster failures, and other errors). A multiple revolution procedure has been examined by Prussing and successfully applied to the case of two-impulse rendezvous with a target in the same circular orbit.[14] For other force models (non-Keplerian), the situation appears more complex. In fact, these singularities (in $\Phi_{rv}$) might be the cause of "spikes" in the $\Delta v$ cost observed in targeting/optimization schemes that utilize the $\Phi_{rv}$ STM block.[24]

## Test Cases

The primer vector theory described in this paper was implemented in an "in-house" Primer Vector Analysis Tool (**PVAT**) to optimize a non-optimal reference trajectory. PVAT was developed in MATLAB® and has a fully automated algorithm. Two sample cases are considered in the 2BP. Plots are expressed as a function of elapsed time in seconds from the initial burn.

### Orbit Initialization

In this case, PVAT is utilized to optimize an orbit initialization for the Leonardo mission concept[25] without any consideration of the formation flying constraints. The orbital elements (semi-major axis, eccentricity, inclination, right ascension of the as-

cending node, argument of perigee, true anomaly) for the initial and final Leonardo orbits are: (6803.1, 0.0017, 1.5084, 278.4, 329.59, unspecified), and (6802.8, 0.0012, 3.6042, 0256.79, 284.27, 184.19), where the semi-major axis is in kilometers and all angles are in degrees. With a two-burn Lambert arc as an initial guess, FreeFlyer™ is used to vary the position of the first maneuver in the departure orbit and the transfer time of flight such that the fuel cost of the transfer to the final orbit is reasonable (< 1 km/s). With this procedure, an initial trajectory with an initial true anomaly of 40 degrees, a time of flight of about 20 minutes and an initial cost of 323 m/s was selected. Figure 3 shows the primer vector data for this reference trajectory. Note that, by inspection of Figure 3, a decrease in the total $\Delta v$ can be achieved by moving the initial departure point. Once this is done, the final optimal primer vector history is plotted in Figure 4. In Figure 5 the total $\Delta v$ history for each iteration is shown. Interestingly, while varying the endpoints, there was an option to switch from a Lambert type I to a Lambert type II transfer arc. A type I/type II arc has a transfer angle less/greater than 180 degrees. The results presented in Figure 4 are for a two-burn type I transfer where a choice was made to continue the iteration instead of switching the Lambert type. Figure 6 displays a plot of the primer vector data right after switching to a type II, which is equivalent to switching to a different initial guess. Right after switching to a type II transfer, the primer vector history indicates that adding an impulse will improve the total trajectory cost. After several iterations, PVAT converges to a 3-burn optimal trajectory with a total cost of 283 m/s (Figure 7). Figure 8 displays the total $\Delta v$ history for this case.
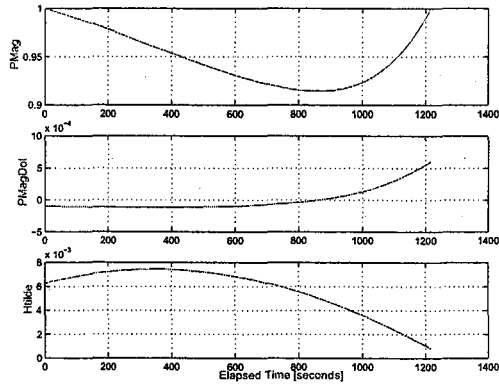
8

Fig. 3   Initial: $\Delta v_{\text{total}} \approx 323$ m/s
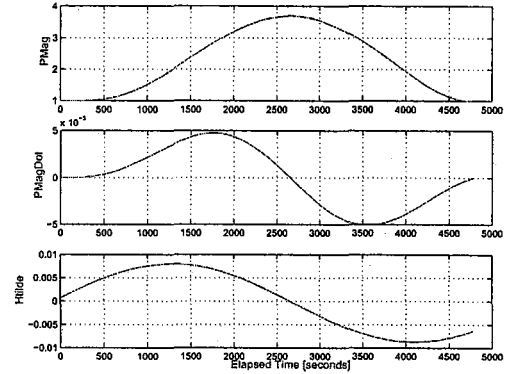


Fig. 6   Type II: $\Delta v_{\text{total}} \approx 295$ m/s
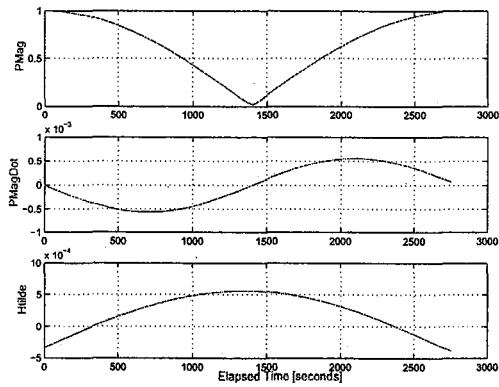


Fig. 4   Final: $\Delta v_{\text{total}} \approx 283$ m/s
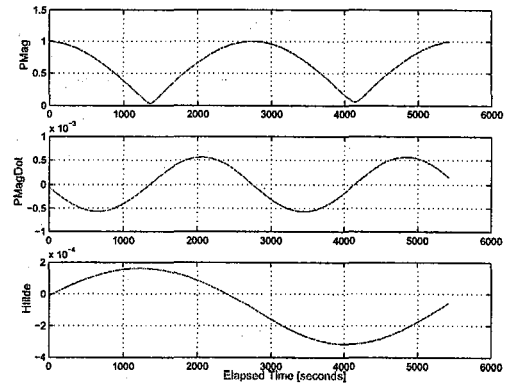


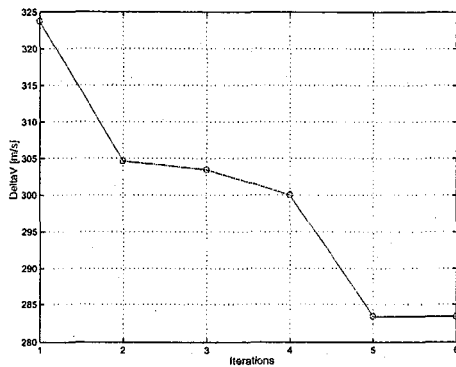Fig. 7   Final: $\Delta v_{\text{total}} \approx 283$ m/s



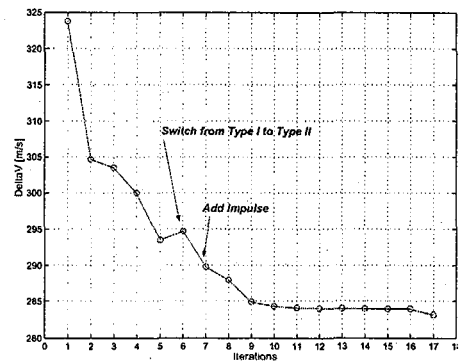Fig. 5   $\Delta v_{\text{total}}$ [m/s] vs Iterations



Fig. 8   $\Delta v_{\text{total}}$ [m/s] vs Iterations

## Line of Apsides Rotation

Next, PVAT is used to analyze a rotation of the line of apsides. In this scenario, the line of apsides should be rotated by 90 degrees. The orbital elements (semi-major axis, eccentricity, inclination, right ascension of the ascending node, argument of perigee, true anomaly) for the initial and final orbits are: (45763.14, 0.672473, 0, 0, 180, unspecified), and (45763.14, 0.672473, 0, 0, 270, unspecified), where the semi-major axis is in kilometers and all angles in degrees. Thus, the orbit shape remains identical, only the argument of perigee changes. There is an additional challenge for this mission as the chosen orbit is highly eccentric compared to the initialization example. Nevertheless, no computational issues appear since between maneuvers the STM propagation holds and no isolated singularities are encountered. Initial guesses (with two-impulses) based on analysis by Lawden[26] are considered. Two different semi-major axis values are used for the initial guesses (i.e., different times of flight). The initial guess with the lower semi-major axis is referred to as initial guess number 1. The trajectory with the higher semi-major axis is referred to as initial guess number 2. Initial guess number 1 (with a shorter time of flight) has a total $\Delta v$ of 3.636 km/s. For this case, the primer vector data in Figure 9 indicates that the fuel expense can be improved. After several iterations of PVAT, where two impulses were added to the trajectory, the code converges to a optimal four-impulse transfer with a total $\Delta v$ of 1.876 km/s (about 52% decrease). The optimal primer vector data is displayed in Figure 10. Figure 11 illustrates the impulsive fuel cost as a function of the PVAT iterations. Now, initial guess number 2, is almost optimal according to the primer vector data illustrated in Figure 12 with a total $\Delta v$ of 1.536 km/s (about 18% lower than the optimal four-burn solution computed for initial guess number 1). This example illustrates that, in general, any solution computed using primer vector theory is a local optimum and, therefore, highly dependent on the initial guess.

## Conclusions

In this investigation, interest is in applying, testing, and extending primer vector theory to create robust software tools that can be used for the new set of upcoming challenging missions. As a result, the range of applicability and some possible numerical problems have been discussed. The theory was also outlined and applied to some sample cases. When applicable, it is clear that primer vector theory is a quick and efficient method to minimize spacecraft fuel usage. Nevertheless, depending on the initial
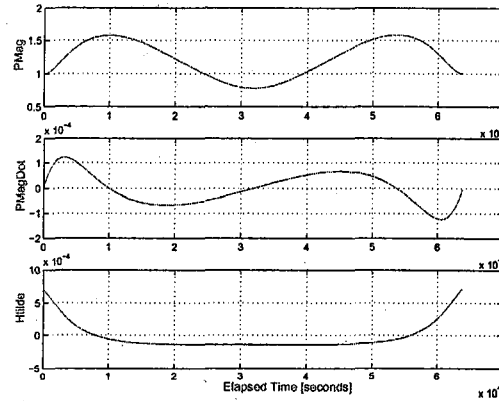


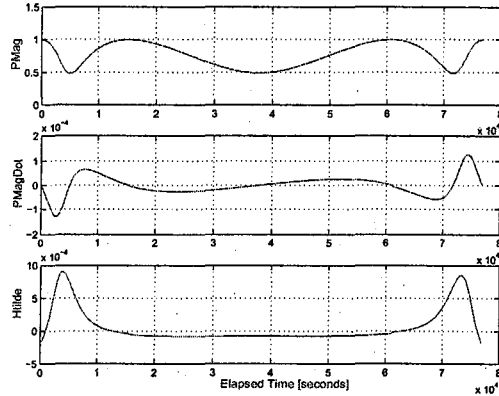**Fig. 9    Guess no.1: $\Delta v_{\text{total}} \approx 3.636$ km/s**



**Fig. 10    Final: $\Delta v_{\text{total}} \approx 1.876$ km/s**
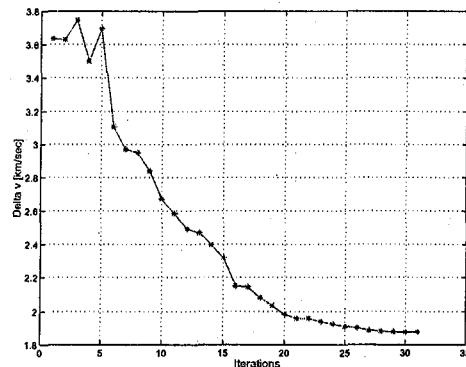


**Fig. 11    $\Delta v_{\text{total}}$ [km/s] vs Iterations**

guesses provided, a particular problem might have multiple locally optimal solutions (with different fuel costs). This, of course, highlights the local optimality of this technique. Also, since primer vector theory is a byproduct of the Calculus of Variations, success is dependent on the existence of other solutions in the neighborhood of the initial guesses. As a result, further research could include utilizing a stochastic method, such as Genetic Algorithms
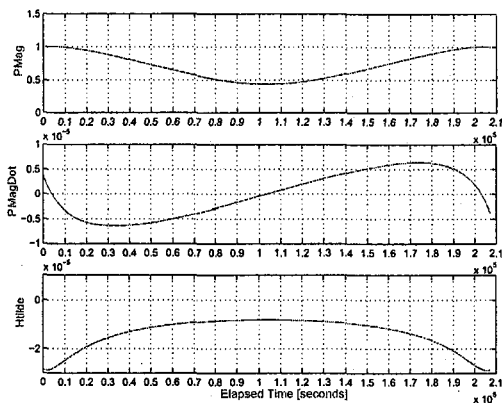
**Fig. 12  Guess no.2:** $\Delta v_{total} \approx 1.536$ km/s (almost optimal)

and/or Simulated Annealing, to increase the probability of finding a global solution by driving the generation of initial guesses. Furthermore, in the two-body problem, investigations of the applicability of primer vector theory to multiple revolution orbits (including high eccentricities) is of interest. Also, the application of primer vector theory to formation flying missions should be investigated.

## Acknowledgments

## References

[1]D. Lawden, *Optimal Trajectories for Space Navigation.* London: Butterworths, 1963.

[2]J. Breakwell, "The Optimization of Trajectories," *Journal of the Society for Industrial and Applied Mathematics,* Vol. 7, June 1959, pp. 215–247.

[3]G. Leitmann, "On a Class of Variational Problems in Rocket Flight," *Journal of the Aeropace Sciences,* Vol. 26, No. 9, 1959.

[4]P. Lion and M. Handelsman, "Primer Vector on Fixed-Time Impulsive Trajectories," *AIAA Journal,* Vol. 6, January 1968, pp. 127–132.

[5]D. Jezewski and H. Rozendaal, "An Efficient Method for Calculating Optimal Free-Space N-Impulse Trajectories," *AIAA Journal,* December 1967, pp. 2160–2165.

[6]D. Jezewski and N. Faust, "Inequality Constraints in Primer-Optimal, N-Impulse Solutions," *AIAA Journal,* Vol. 9, April 1971, pp. 760–763.

[7]D. Jezewski, "Primer Vector Theory and Applications," NASA Johnson Space Center, Technical Report, Houston, Texas, November 1975. NASA TR R-454.

[8]J. Prussing, "Optimal Four-Impulse Fixed-Time Rendezvous in the Vicinity of a Circular Orbit," *AIAA Journal,* Vol. 7, May 1969, pp. 928–935.

[9]J. Prussing, "Optimal Two- and Three-Impulse Fixed-Time Rendezvous in the Vicinity of a Circular Orbit," *AIAA Journal,* Vol. 8, July 1970, pp. 1221–1228.

[10]J. Prussing and J. Chiu, "Optimal Multiple-Impulse Fixed-Time Rendezvous in the Vicinity of a Circular Orbit," *Journal of Guidance and Control,* Vol. 9, January-February 1986, pp. 17–22.

[11]L. Wellnitz and J. Prussing, "Optimal Trajectories for Time-Constrained Rendezvous Between Arbirary Conic Orbits," *AAS/AIAA Astrodynamics Specialists Conference,* Kalispell, Montana, August 10-13 1987. AAS Paper 87-539.

[12]D. Taur, J. Prussing, and V. Coverstone-Carroll, "Optimal Impulsive Time-Fixed Orbital Rendezvous and Interception with Path Constraints," *Journal of Guidance, Control, and Dynamics,* Vol. 18, January-February 1995, pp. 54–60.

[13]J. Prussing, "Optimal Impulsive Linear Systems: Sufficient Conditions and Maximum Number of Impulses," *Journal of the Astronautical Sciences,* Vol. 43, AprilJune 1995, pp. 195–206.

[14]J. Prussing, "A Class of Optimal Two-Impulse Rendezvous Using Multiple Revolution Lambert Solutions," *Journal of the Astronautical Sciences,* April-September 2000, pp. 131–148.

[15]L. Hiday, *Optimal Transfers Between Libration-Point Orbits in the Elliptic Restricted Three-Body Problem.* Ph.D. Dissertation, Purdue University, West Lafayette, Indiana, August 1992.

[16]K. Howell and L. Hiday-Johnston, "Transfers Between Libration Points in the Elliptic Restricted Three Body Problem," *Celestial Mechanics and Dynamical Astronomy,* Vol. 58, April 1994, pp. 317–337.

[17]J. Prussing and B. Conway, *Orbital Mechanics.* New York: Oxford University Press, 1993.

[18]S. Citron, *Elements of Optimal Control.* Holt, Rinehart and Winston, 1969.

[19]K. Howell and H. Pernicka, "Numerical Determination of Lissajous Trajectories in the Restricted Three Body Problem," *Celestial Mechanics,* Vol. 41, 1988, pp. 107–124.

[20]K. Richon and M. Mathews, "An Overview of the MAP Trajectory Design," *AAS/AIAA Astrodynamics Specialists Conference,* Sun Valley, Idaho, August 1997. AAS Paper 97-728.

[21]T. Goodson, "Monte-Carlo Maneuver Analysis for the Microwave Anisotropy Probe," *AAS/AIAA Astrodynamics Specialists Conference,* Quebec City, Canada, JPL, July 30-August 2 2001. AAS 01-331.

[22]R. Stern, "Singularities in the Analytic Solution of the Linearized Variational Equations of Elliptical Motion," Experimental Astronomy Lab., Massachusetts Institute of Technology, Technical Report, Cambridge, Massachusetts, May 1964. Report RE-8.

[23]R. Farquhar, "Halo-Orbit and Lunar Swingby Missions of the 1990's," *Acta Astronautica,* Vol. 24, 1991, pp. 227–234.

[24]R. Wilson, K. Howell, and M. Lo, "Optimization of Insertion Cost for Transfer Trajectories to Libration Point Orbits," *AIAA/AAS Astrodynamics Specialists Conference,* Girdwood, Alaska, August 16-19 1999. AAS 99-041.

[25]S. Hughes and L. Mailhe, "A Preliminary Formation Flying Orbit Dynamics Analysis for Leonardo-BRDF," *2001 IEEE Aerospace Conference,* Big Sky, Montana, March 10-17 2001. Paper 905.

[26]D. F. Lawden, *Impulsive Transfer Between Elliptic Orbits,* pp. 323–351. Optimization Techniques, New York: Academy Press, 1962. edited by G. Leitman.